

光学学报

无人机载污染气体激光监测技术的研究进展

王刚^{1,2}, 武红鹏^{1,2}, 廖洁麟³, 魏永峰³, 乔建波³, 董磊^{1,2*}

¹山西大学量子光学与光量子器件国家重点实验室, 激光光谱研究所, 山西 太原 030006;

²山西大学极端光学协同创新中心, 山西 太原 030006;

³山西迪奥普科技有限公司, 山西 太原 030006

摘要 讨论无人机载污染气体激光监测技术的发展现状以及在我国“天地空”一体化监测体系中的应用价值。无人机载污染气体激光监测平台由无人机平台和机载污染气体激光传感器两部分组成。从无人机平台出发, 首先介绍当前无人机平台的类型, 阐明不同类型无人机的优势和劣势; 然后, 介绍适用于无人机装载的几种激光光谱传感技术原理和相关应用, 讨论无人机载污染气体激光监测技术在气体监测领域的应用潜能。

关键词 激光光谱; 激光传感器; 无人机; 气体监测

中图分类号 O433.1; O659.21

文献标志码 A

DOI: 10.3788/AOS230504

1 引言

随着工业的快速发展以及人民生活水平的不断提升, 我国许多地区面临着大气环境质量改善的巨大压力。目前, 我国正在积极建设“天地空”一体化监测体系, 以满足环境综合监测等方面的迫切需求。“天”上有大气和陆地综合观测卫星, “地”面布控大量的空气质量监测站, 对“空”的监测往往借助于飞机或热气球。然而, 对于距离地面 0.1~1 km 的地表边界层, 传统的监控平台很难覆盖。这是因为飞机由于安全原因无法在人口或工业密集区进行低空飞行, 卫星数据无法提供污染气体的垂直高度信息, 而且在污染气体溯源上也无法满足横向空间分辨率要求, 而热气球仅仅能够提供单点位置的垂直数据信息。因此, 在环境监控方面, 我国亟需发展对“空”监控的新技术、新装备。

近年来, 全国化工企业重大安全事故频发, 天津港、四川江安、河北张家口、江苏响水、河南义马等地的多起化工厂爆炸事故, 使人民的生命财产遭受了巨大损失。这些化工企业经常建在偏远的地区, 受基础设施的限制, 在厂区附近建设地面监测站的成本较高, 但效果不佳。车载的移动式激光遥测监控往往会受到厂区内建筑物或生产设备的阻挡。因此, 化工厂的安全检查除了法规的完善, 更离不开具有高科技含量的监测监管手段。

无人机以其机动性强、飞行高度适中等特点, 很容

易实现对地表边界层的监测, 完善“天地空”一体化监测体系。最初研制无人机大多是基于军事用途, 或是为了代替航空人员执行一些危险性高的任务, 后来逐渐用于民生和科研领域, 例如地球科学考察、大气取样、农田植被监测、地图测绘等, 并展现出巨大的潜能^[1-6]。至今, 各种无人机平台出现在人们的视野, 包括固定翼无人机^[7-9]、直升无人机^[10-12]、伞翼无人机^[13-15]、垂直升降无人机^[16-18]等。然而, 影响无人机现场应用的最主要因素是无人机续航能力不足、单一无人机效率低下, 因此利用多架无人机协同工作完成预期的任务是当前无人机的主要发展方向^[19]。

由于无人机的续航时间较短, 机载气体传感器在实现高灵敏度、高选择性的同时, 必须满足轻质量、小体积、低功耗的要求。当前用于无人机平台的痕量气体传感器类型主要分为电化学型、光致电离型、催化燃烧型和红外传感型。前 3 种类型的质量轻、体积小、功耗低, 优势明显, 符合无人机对载荷的要求, 但气体选择性差的缺点也很突出。红外传感器依靠气体独特的指纹光谱来区分和探测目标气体, 与窄线宽的激光器连用将同时具有高灵敏度、高分辨率和高选择性特征, 显著减少对测量的误判, 满足无人机平台对污染气体监测以及污染源定位的要求^[20-25], 但是需要对其结构进行改造, 以满足无人机平台对其体积、质量和功耗的要求。随着激光技术的发展, 各种类型的激光器应运而生, 极大地推动了频谱技术的发展。目前, 已经公开

收稿日期: 2023-02-03; 修回日期: 2023-03-09; 录用日期: 2023-04-03; 网络首发日期: 2023-05-08

基金项目: 国家重点研发计划(2019YFE0118200)、国家自然科学基金(62235010, 62175137, 62122045, 62075119)、山西省杰出青年基金(20210302121003)

通信作者: *donglei@sxu.edu.cn

报道了许多基于激光传感技术的小型传感器,尤其是微纳加工技术的不断改进,使得光学传感器核心部件的体积越来越小、功耗越来越低,而测量精度越来越高,从整体上进一步缩小了激光气体传感器的体积。

本文从无人机平台和激光气体传感器出发,分别介绍当前无人机平台的类型以及适用于无人机装载的几种激光传感技术的原理,阐明不同类型无人机的优劣以及无人机电载激光传感技术的应用,并讨论无人机电载污染

气体激光监测平台在气体监测领域的应用潜能。

2 无人机平台类型

随着科技的发展,市场上出现了各式各样性能不同的无人机,以满足不同种类的任务需求。无人机种类划分有着不同的标准,图 1 列出了按空气动力学原理、升降方式和尺寸性能(无人机基本尺寸以及飞行高度和续航能力)进行划分的结果^[26-36]。

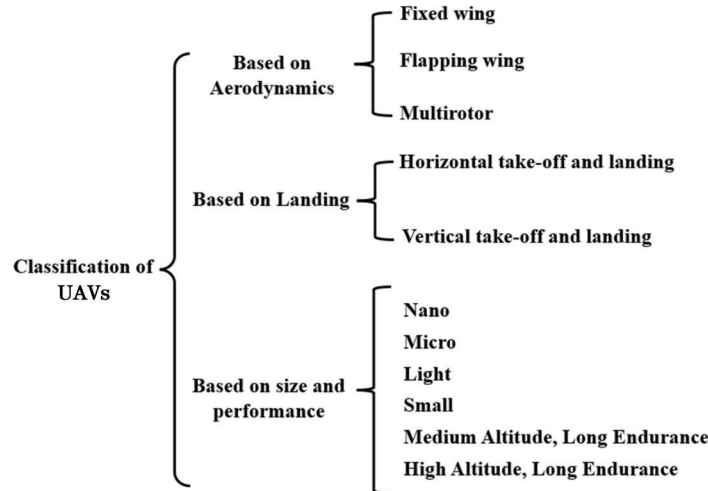


图 1 无人机按空气动力学原理、升降方式和尺寸性能的分类结果^[26-36]

Fig. 1 Classification results of UAVs based on aerodynamics, landing, size, and performance^[26-36]

基于空气动力学原理,无人机可分为固定翼(fixed wing)无人机、旋翼(multirotor)无人机、扑翼(flapping wing)无人机。固定翼无人机的起飞方式为手抛起飞或者弹射起飞,这两种方式都需要借助外力,所以这类无人机的缺点是无法实现悬停姿态且对起飞环境有较高要求,优点是拥有较强的续航能力和高速飞行能力,可用于执行大范围、高速的侦察和监测任务^[27-28]。直升无人机是固定翼无人机和旋翼无人机的结合,采用旋翼提供升力,具有垂直起降能力,能够在狭小的空间内起降,适合执行低空近距离侦察和监测任务,但是续航时间较短,飞行速度较慢^[10-12]。扑翼无人机的设计灵感主要来自小型蜂鸟和大型蜻蜓等昆虫,用扑翼模拟鸟类和昆虫的翅膀,通过振动扑翼产生无人机所需的升力^[29-31]。目前扑翼无人机的相关技术还非常不成熟,几乎没有进入实用市场。旋翼无人机的优势是具有垂直升降的能力,可以在相对苛刻的起飞条件下起飞,可以在某个位置定高、悬停等飞行姿态,有助于采集数据和提高时空分辨率,这就使得它们成为环境监测的理想无人机^[32-33]。旋翼无人机的缺点是采用锂电池供电,这就使得该类型无人机的负载能力和续航能力有限。

按平台升降方式,无人机可分为水平升降(HTOL)无人机和垂直升降(VTOL)无人机。水平升降无人机的典型代表是固定翼无人机,它们的巡航速

度快、着陆平稳,但不能实现悬停滞留等飞行姿态,且需要跑道来起飞和降落,成本相对高;垂直升降无人机的典型代表是旋翼无人机,优点是其布控便携,无需跑道辅助起飞,能实现垂直飞行、降落和悬停等飞行姿态,且可用于远程操控和复杂地形勘测,成本相对较低^[34-35]。

按平台尺寸性能(质量、飞行高度和续航时间),无人机可划分为纳米型(nano)无人机、微型(micro)无人机、轻型(light)无人机、小型(small)无人机、中空长续航(MALE)无人机以及高空长续航(HALE)无人机^[26,36]。表 1 列出了基于尺寸性能划分的无人机类别^[36-39]:纳米型无人机和微型无人机的体积小,一般在低高度飞行,受电池的质量和尺寸限制,其飞行时间为 5~30 min;轻型无人机由于其尺寸更大,便于搭载容量更大的电池,因此其飞行高度更高,续航时间更长;小型无人机包括低空短续航(LASE)无人机、低空长续航(LALE)无人机,LASE无人机的结构经过优化设计便于现场部署、回收和运输,但考虑到质量和性能之间的平衡,其续航时间通常被限制在 1~2 h,通信距离在距地面站几千米以内,而 LALE 无人机可以在几千米的高度长时间携带几千克的有效载荷;MALE 无人机通常比低空级别的无人机大得多,普遍在距离地面站数百千米的范围内飞行,高度可达 9 km,续航时间长达数小时;HALE 无人机是最大、最复杂的无人

机,比许多通用航空有人驾驶飞机大,这些无人机可以在 20 km 或更高的高度飞行,执行延伸数千千米的任

务,续航时间长达十几小时。

表 1 基于尺寸性能的无人机分类^[36-39]
Table 1 Classification of UAVs based on size and performance^[36-39]

Type of UAVs	Maximum mass /kg	Maximum range / km	Maximum altitude / km	Flight duration /h	Category of UAVs
Nano	0.2	5	0.3	0.05-0.17	Fixed wing/multirotor
Micro	2.0	25	1.5	0.17-0.50	Fixed wing/multirotor
Light	50.0	70	3.0	0.50-1.00	Fixed wing/multirotor
Small	150.0	150	5.0	1.00-2.00	Fixed wing
MALE	1000.0	200	9.0	5.00-9.00	Fixed wing
HALE	1000.0	250	20.0	10.00-20.00	Fixed wing

综上所述,在无人机载污染气体监测中:如果考虑低成本,选用微型无人机是最合适的,且微型无人机包括固定翼无人机和旋翼无人机;考虑到污染气体监测区域无人机的起飞环境以及数据采集监测和时空分辨率的关系,选用具有悬停和低速飞行性能的旋翼无人机比较合适,当然也可选用固定翼式垂直升降无人机,但该类型无人机的成本较高。旋翼无人机又分为单旋翼、三旋翼、四旋翼、六旋翼和八旋翼无人机,其中考虑到多无人机协调合作效率以及“炸机”风险,选用四旋翼或者六旋翼无人机比较合适。由于旋翼无人机普遍采用可充电电池,因此其缺点是续航时间短,这样在无人机污染气体激光监测平台中气体传感器就需要满足小体积、轻质量、低功耗和高灵敏度的要求。

3 无人机载激光传感技术

无人机的续航问题对机载气体传感器提出了小体积、轻质量、低功耗的要求。红外光学气体传感器依靠气体独特的指纹光谱来区分和探测目标气体,如果和窄线宽的激光器连用,将同时具有高灵敏度、高分辨率和高选择性特征,缺点是体积大、质量重。随着现代微加工技术的发展,许多光学驱动元件以及电学元件可以做到很小的尺寸,激光器种类的多样性也极大地推进了无人机载激光气体传感器发展,许多微型光学传感模块的有效性在痕量气体监测领域已被实验验证^[40-45]。本节将介绍适用于无人机的激光气体传感技术原理与应用,涉及直接吸收光谱技术和间接吸收光谱技术两大类。

3.1 直接吸收光谱技术

直接吸收光谱技术是通过分别测得初始光强信号和经过待测气体的光强信号来反演气体分子浓度信息的技术^[20-22,46-48]。直接吸收光谱技术的原理为朗伯-比尔定律,当一束光通过待测气体时,一部分能量被气体吸收,在不考虑散射的情况下,入射光的能量等于出射光的能量与被测气体吸收能量之和。初始强度为 $I_0(\nu)$ 的光经过长度为 L 的气体样品后,透射光强 $I_t(\nu)$ 可表示为

$$I_t(\nu) = I_0(\nu) \exp[-\alpha(\nu)CL], \quad (1)$$

式中: α 为吸收气体系数; C 为气体分子浓度; ν 为激光频率。在具体的操作过程中,若选用的光源为单色光源,则被测物质的直接吸收光谱可以通过探测透射光强度随光源波长或频率的变化曲线来获得,典型的代表为可调谐二极管激光吸收光谱(TDLAS)技术;若光源为宽带光源,则需要对入射光或者透射光在频域上进行分光才能获得相应的直接吸收光谱,典型的代表为非色散红外(NDIR)技术。

基于可调谐二极管激光吸收光谱技术的痕量气体检测方法具有分辨率高和响应速度快的优点,可用于目标气体分子浓度在线监测。它经常和波长调制光谱(WMS)技术相结合来降低噪声、提高信噪比。波长调制光谱技术是用相对较高的频率(kHz)调制激光的波长,并在调制频率或该频率的整数倍处解调吸收谱信号,并进行评估和分析,从而得到气体分子浓度。由于粉红噪声即 $1/f$ 噪声的影响主要存在于低频段,而波长调制光谱技术将吸收光谱的检测转移到具有低噪声本底的高频段,因此提高了在嘈杂环境下可调谐二极管激光吸收光谱的信噪比。由式(1)可知,可调谐二极管激光吸收光谱技术产生的信号幅值分别与激光的功率、气体吸收线强度和光学吸收路径长度成正比。为了在一定的空间情况下获得较长光学吸收路径,通常使用一种叫作多通池的光学器件,它由两块或多块镜片组成,使光在镜片间来回反射,以达到增长光程的效果^[18-21,43-45]。在一个可调谐二极管激光吸收光谱气体传感器中,体积最大的光学器件是多通池,因此发展无人机载可调谐二极管激光吸收光谱气体传感器的关键在于小型化多通池。

近年来,小型化多通池设计受到广泛关注。2016年,Dong等^[47]报道了一种物理尺寸为 $17\text{ cm} \times 6.5\text{ cm} \times 5.5\text{ cm}$ 的密集光斑模式多通池(MPC),其有效光程为 54.6 m ,把它和一个带间级联(ICL)激光器联用,可实现最小检测限为 5×10^{-9} 的 CH_4 检测,整机功率仅为 3.7 W 。2018年,Cui等^[48]采用波长为 $2.33\text{ }\mu\text{m}$ 的分布式反馈(DFB)二极管激光器和光学路

径长度为 14.5 m 的赫里奥特型多通池, 实现了 10^{-6} 量级的 CO 检测。2020 年, Cui 等^[42]设计了一种基于三维 (3D) 打印光纤耦合且免校准的迷你型多通池, 其物理尺寸为 $4\text{ cm} \times 4\text{ cm} \times 6\text{ cm}$, 容积为 20 mL, 有效光程为 4.2 m, 实物如图 2 所示。它结合 $1.65\text{ }\mu\text{m}$ 的 DFB 激光器, 实现了最小检测限为 117×10^{-9} 的 CH_4 探测。迷你型多通池的发展极大地促进了可调谐二极管激光吸收光谱气体传感器的小型化, 再结合小尺寸的近红外 DFB 激光器和激光驱动板, 辅以锁相放大板, 即可实现小型化的机载传感器集成。

对于可调谐二极管激光吸收光谱技术来说, 光电探测器是必不可少的元件, 它的波长工作范围和响应带宽受到技术、工艺、设计、材料的限制。最近, 利用音叉式石英晶振的压电效应设计光热探测器的研究受到

广泛关注, 目前已经证明了石英音叉可以作为窄带宽 (1 Hz)、快速响应 (几十 kHz)、宽波长工作范围的红外光热探测器, 适用于可调谐二极管激光吸收光谱技术^[49-50]。如图 3 所示, 该传感器以石英音叉为热探测器, 与小型化多通池组成一个尺寸为 $78\text{ mm} \times 40\text{ mm} \times 40\text{ mm}$ 的紧凑传感模块, 使用 $1.65\text{ }\mu\text{m}$ 的 DFB 激光器作为光源, 实现了最小检测限为 52×10^{-9} 的 CH_4 探测, 并通过连续一周的 CH_4 分子浓度监测实验验证了该传感器的可靠性。基于光热效应的音叉式石英晶振热探测器体积小、成本低, 适合代替可调谐二极管激光吸收光谱技术中相对昂贵的光电探测器, 但是音叉式石英晶振热探测器在低气压下的信号比常压下要好, 在小型化、轻质量和高灵敏度之间取得平衡是音叉式石英晶振热探测器面临的问题。

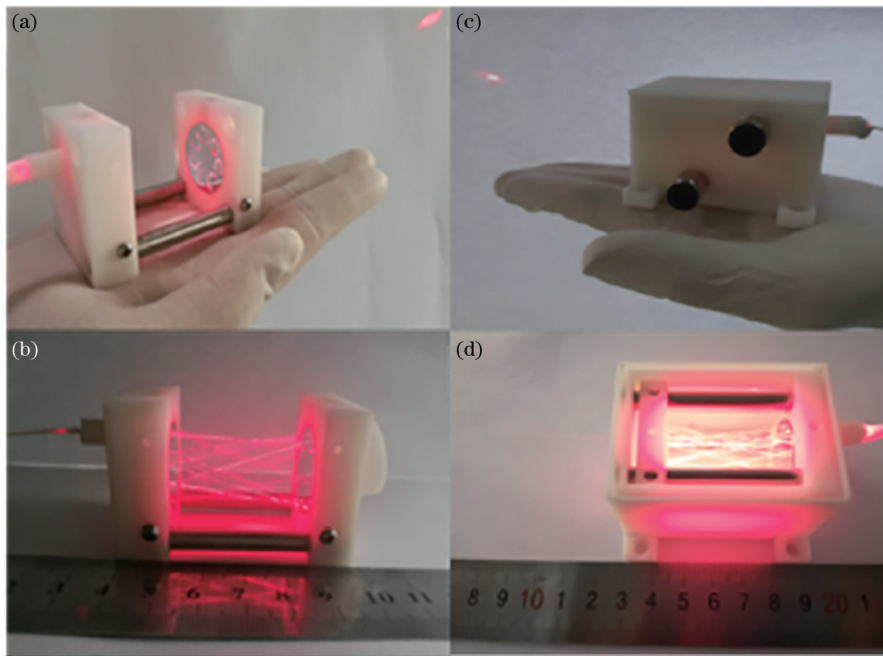


图 2 三维打印的迷你多通池实物图^[42]。(a)七个不相交圆圈密集光斑模式;(b)两个球面镜间光线轨迹;(c)带有进气口和出气口的迷你多通池;(d)迷你多通池俯视图

Fig. 2 Photographs of 3D printed mini-MPC^[42]. (a) Seven nonintersecting-circle spot pattern; (b) ray trajectories between two spherical mirrors; (c) mini-MPC with a gas inlet and an outlet; (d) top view of the mini-MPC

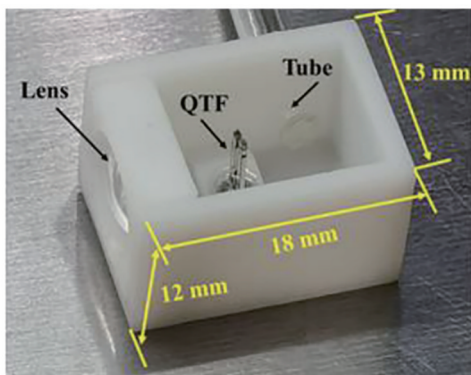


图 3 音叉式石英晶振热探测器的照片^[50]

Fig. 3 Photograph of QTF-thermal detector^[50]

非色散红外技术也是直接吸收光谱技术的一种, 它利用气体分子吸收特定波长的红外辐射后产生的热效应变化, 将这种热信号通过热释电探测器转化为可测量的电流信号, 以此测定该气体的分子浓度。该方法常用于分析对红外辐射有较强吸收性能的气态物质, 如一氧化碳、二氧化碳、甲烷、氨气等^[51]。它采用的光源通常是廉价的非相干光源, 比如灯泡, 其光源发出的光经过气体池后入射到滤光片上进行分光, 最后入射到热释电探测器, 得到所需波段的光吸收信息, 从而反推出气体的分子浓度。由于从光源发出的、经过气体池的光线是复合的、非分散的, 因此这种测量方式被称为非分散红外技术。这种技术由于微型设备的发展

而得到了广泛的应用,尤其是被应用到某些常见气体的大批量、低成本测量中,例如二氧化碳,目前已设计出各种各样的气体池^[52-53]。图 4 显示了一种测量二氧化碳的非色散红外传感器,它是一个直径为 20 mm、高

为 16.5 mm 的圆柱体。该传感器体积小,适合作为机载传感器,但是较短的光学吸收路径限制了它的最小检测限,因此大多用于测量吸收线较强的气体分子浓度^[43]。

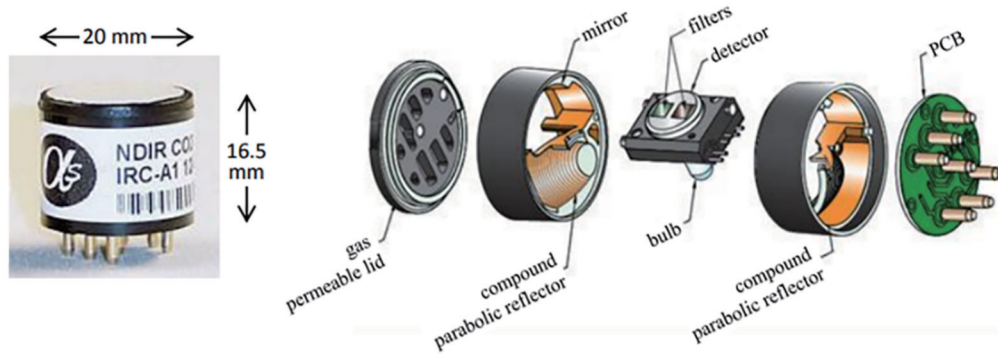


图 4 非分散红外传感器外部和内部图^[43]

Fig. 4 External and internal images of non-distributed infrared sensor^[43]

3.2 间接吸收光谱技术

间接吸收光谱技术是通过测量目标气体与激光相互作用后产生的热、声、光等信号来反演气体分子浓度信息。光声光谱技术是间接吸收光谱技术的一种。在光声光谱技术中,激光通过被测气体后,气体分子吸收激光能量跃迁至高能级,通过无辐射跃迁回基态来释放能量,调制的激光会使气体分子周期性地吸收、释放热量,导致分子局部温度升降,进而产生声波。传统的光声光谱技术采用宽带麦克风来探测声音信号,这就导致探测带宽内过多的无用噪声被探测到^[54-55]。石英增强光声光谱(QEPAS)技术是近几年才发展起来的一种新型光声光谱技术,其显著特点是使用音叉式石英晶振代替传统光声光谱中的宽带麦克风来实现对微弱光声信号的探测,在石英增强光声光谱技术中,音叉式石英晶振是关键部件,它利用石英材料的压电效应将声波引起的机械振动转化为电信号,然后使用跨阻抗前置放大器进行放大。这种小尺寸的音叉式石英晶振的典型谐振频率为 32.768 kHz,品质因子很高,在真空封装中品质因子高达 100000,在常压下为 10000 左右,常被用于石英表的频率标准^[56-57]。该技术不但保留了传统光声光谱技术所具有的零背景、无波长选择性、信号幅值正比于激励光功率的特点,而且拥有品质因数高、响应带宽窄、对环境噪声免疫的优点,以及体积小、结构紧凑以及成本低的优势^[56-60]。

光声信号的强度表达式为

$$S_{PA} = C_j(\omega_j)\alpha P_0, \quad (2)$$

式中: S_{PA} 为光声信号; C_j 为腔的常数; P_0 为激发光功率; α 为气体吸收系数; ω_j 为声波频率。显然,信号强度正比于气体吸收系数和激发光功率,因此,常选用对应气体吸收系数强的中红外波段激光器来增强光声信号,或使用光纤放大器来提高激光功率,以达到增强光声信号的目的^[57-62]。在石英增强光声光谱技术中,光

声探测模块由光谱测声器和气室组成,气室仅用于为光谱测声器创建一个与外界环境隔离的气体环境,光谱测声器是石英增强光声光谱传感器的核心器件,光谱测声器由音叉式石英晶振和微型声音谐振腔组成,即在石英音叉上安装一个声学微谐振器来限制声波,并通过它们之间耦合声波来提高声波强度。目前已经开展了大量有关音叉式石英晶振设计和微谐振器参数优化的工作^[58-63]。Wei等^[64]报道了一款用于近红外DFB激光器的光纤耦合式光声探测模块,如图5所示。该模块使用标准音叉式石英晶振,物理尺寸仅为 20 mm×12.7 mm×8.5 mm,该模块包括近红外DFB激光器、小型化激光驱动、跨阻抗前置放大器以及锁相放大板,可实现小型化的石英增强光声传感器集成。

石英增强光声光谱中石英音叉的高品质因数特性使得其响应时间达到约 100 ms,加上信号处理时间,系统完成单次数据点测量的时间长达 400 ms,因此无法实现痕量气体的快速检测,而且需要经常对音叉式石英晶振进行频率校准^[56-64]。针对上述问题,Wu等^[65]报道了拍频石英增强光声光谱(BF-QEPAS)技术,如图6所示。该技术是通过快速扫描一束激光的波长,从而产生脉冲声信号,瞬间激励音叉,使其随后自由衰荡,产生瞬态响应。该技术与传统的石英增强光声光谱技术的区别就在于调制频率和激发音叉式石英晶振的响应模式不同。在BF-QEPAS技术中,光源调制频率为 $f_0 \pm \Delta f$,其中 f_0 为共振频率, Δf 为频率偏置,使用一次谐波解调石英晶振的输出信号,可得到拍频信号。拍频信号的幅值正比于目标气体的分子浓度。根据式(3),由拍频信号得到的 Δt 可算出 Δf 。由于调制频率 f 已知,因此可计算得到音叉式石英晶振的共振频率 f_0 。根据式(4),Q值可以通过共振频率 f_0 和从拍频信号获得的衰荡时间 τ 计算得到。

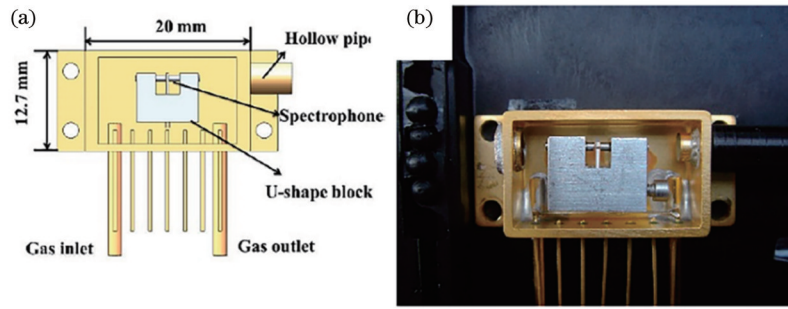


图 5 光纤耦合式光声探测模块^[64]。(a)光声探测模块的 CAD 图；(b)光声探测模块实物图

Fig. 5 Optical fiber coupled photoacoustic detection module^[64]. (a) CAD image of photoacoustic detection module; (b) photo of photoacoustic detection module

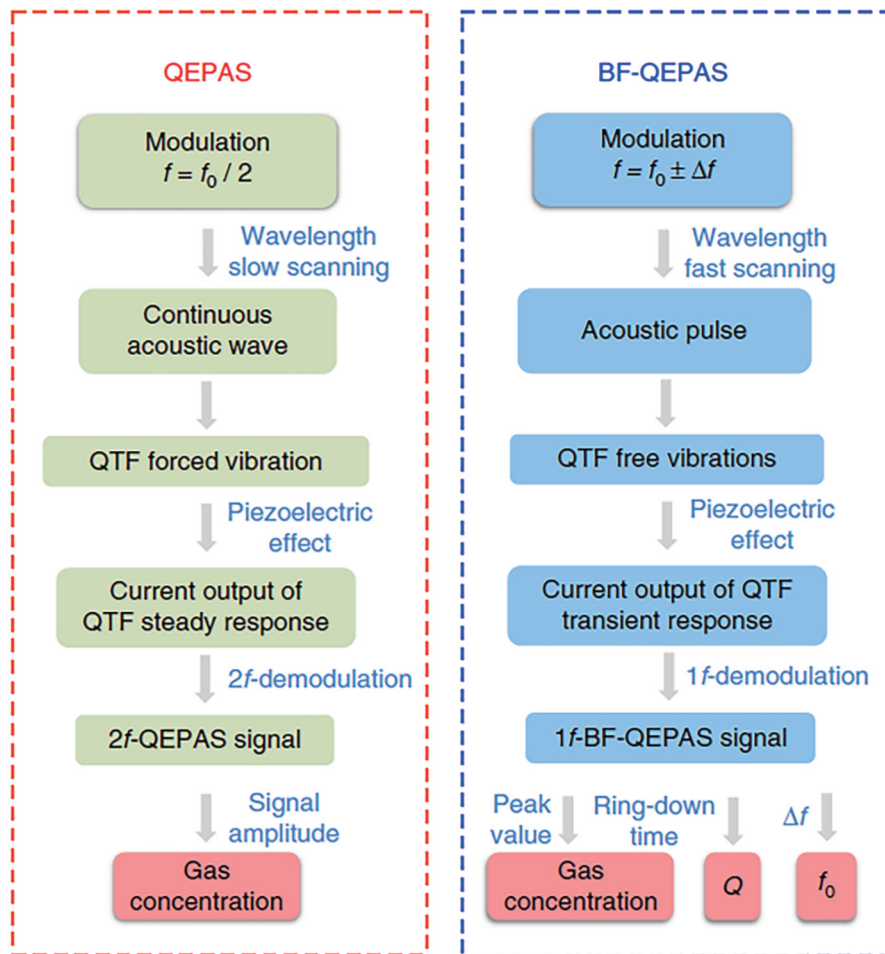


图 6 传统石英增强光声光谱和拍频石英增强光声光谱的比较^[66]

Fig. 6 A side-by-side comparison of conventional QEPAS and BF-QEPAS techniques^[66]

$$\Delta f = \frac{1}{\Delta t} = |f - f_0|, \quad (3)$$

$$Q = f_0 \times \tau. \quad (4)$$

BF-QEPAS 技术可实现对目标气体分子浓度 C 、石英音叉共振频率 f_0 及其品质因数 Q 的同步探测, 从而在快速测量目标气体分子浓度的同时获取校准系统所需的电学参数, 并自动完成相关实验参数的校准, 真正实现了对痕量气体分子浓度的快速、连续监测。Li 等^[67]报道了基于 BF-QEPAS 的应用, 采用 $10.359 \mu\text{m}$ 的中红外 QCL 激光器和 BF-QEPAS 实现了人体呼出

氨气 10^{-9} 量级的检测。基于 BF-QEPAS 的传感器满足机载激光传感器的小体积、轻质量、低功耗、快速响应、免校准的要求, 但需要在近红外波段实现痕量气体高灵敏度探测以及强振动环境下的稳定连续运行。表 2 列出了相应的机载激光监测技术指标。

4 无人机载激光传感系统的应用

图 7 展示了机载传感系统中无人机平台、传感器平台和地面控制站之间相互联系的情况。无人机平台

表 2 机载激光监测技术指标^[40-67]

Table 2 Indicators of airborne laser monitoring technologies^[40-67]

Technique	Size of sensing unit / (cm×cm×cm)	Light source	Detection limit (gas type)
TDLAS	17×6.5×5.5	3.59 μm ICL	3×10 ⁻⁹ (H ₂ CO)
		3.3 μm ICL	5×10 ⁻⁹ (CH ₄)
		3.3 μm ICL	8×10 ⁻⁹ (C ₂ H ₆)
NDIR	4×4×6	1.65 μm DFB	117×10 ⁻⁹ (CH ₄)
	0.2×0.2×0.2	4.2 μm LED	1×10 ⁻⁶ (CO ₂)
		3.3 μm LED	7×10 ⁻⁹ (CO ₂)
	10×4×3	3.3 μm LED	200×10 ⁻⁹ (CH ₄)
QEPAS	0.6×0.14×0.02	0.28 μm LED	200×10 ⁻⁹ (O ₃)
		1.53 μm DFB	85×10 ⁻⁹ (C ₂ H ₂)
		1.53 μm DFB	418×10 ⁻⁹ (NH ₃)
		1.58 μm DFB	734×10 ⁻⁹ (H ₂ S)
		3.34 μm ICL	7×10 ⁻⁹ (C ₂ H ₆)
		4.3 μm QCL	0.3×10 ⁻⁹ (CO ₂)
		4.6 μm QCL	1.5×10 ⁻⁹ (CO)
		5.26 μm QCL	5×10 ⁻⁹ (NO)

上挂载了机载计算机,通过串口(MAVLink通信协议)和无线通信分别连接飞控和笔记本电脑,用于向无人机飞控发送指令和接收笔记本电脑端的命令。传感器平台安装在无人机上,通过数传方式将采集的气体分子浓度信息传输到笔记本电脑。笔记本电脑通过SSH远程连接机载计算机,给无人机发布任务指令,并从地面控制站获取无人机飞行途中的GPS、飞行速

度、高度以及姿态等数据。对这些信息进行后续处理,根据相应的气体扩散模型以及污染源定位算法来完成相应的任务。

无人机在执行任务时,由于极易出现炸机事故,实验成本很高,因此对无人机路径规划代码的模拟验证和起飞前状态参数的检查十分重要。选择适合任务的无人机模拟器、机载计算机和地面控制站可以明显降低执行任务时的容错率。无人机模拟器能为无人机创建一个模拟真实飞行情况的环境,多个基于Ubuntu系统的免费开源模拟器JMAVSim、Gazebo、FlightGear、X-Plane、Air Sim可进行执行任务所需路径规划代码的模拟验证,确保真实飞行时的安全性。表3比较了这些模拟器的开源商用情况、界面是否兼容机器人操作系统(ROS)、动作捕获、障碍物、支持MAVLink通信协议以及开发难易程度^[66,68]。常见的机载计算机有树莓派(Raspberry Pi)、Nvidia TX系列和Odroid。它们之间的区别在于性能、功耗、尺寸、接口和价格不同。Raspberry Pi是一种开源计算机,价格便宜、易于使用,可用于执行轻量级计算任务,并与传感器、电机和其他硬件进行通信,是最受欢迎的机载计算机之一^[69]。Nvidia TX系列计算模块专为机器人、无人机提供高性能计算和机器学习能力,具有低功耗、高性能、强大的图形处理能力,并配置深度学习加速器。Odroid是一种高性能的单板计算机,与Raspberry Pi类似,能提供更快的处理速度和更大的内存,适用于执行计算密集型任务^[70-72]。ArduPilot提供了多个开源地面控制站(QCS)软件,如QGroundControl、Mission Planner和MAVProxy。这些软件能够实时查看无人机的状态参数,确保在起飞前无人机的状态参数是正常的,并且可以在这些软件的基础上进行相应的开发。表4比较了这些地面控制站软件之间的差别^[73-75]。

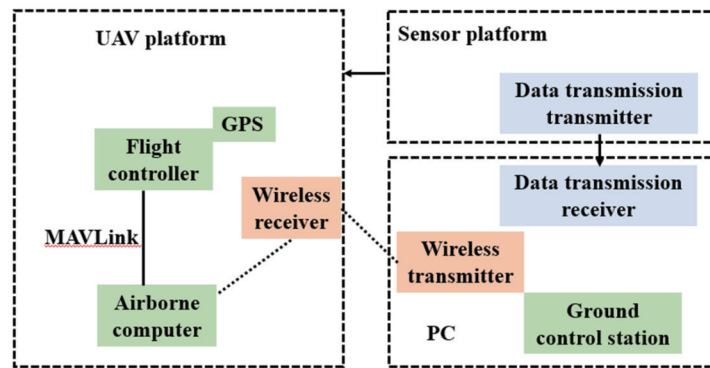


图 7 机载传感系统示意图

Fig. 7 Schematic of airborne sensing system

无人机螺旋桨在转动的过程中产生的湍流是一种高度复杂的三维非稳态、带旋转的不规则流动。在湍流中,空气的各种物理参数(如流动速度、压力、温度等)随时间和空间发生随机变化,从而导致激光气体传

感器输出信号产生波动。为了抑制湍流扰动对无人机周围传感器的影响,需要分析无人机周围的湍流分布,并寻找最优的传感器安装位置。这是无人机飞行时面临的一个复杂问题。Li等^[76]使用ANSYS FLUENT

表 3 可用的无人机模拟器的比较^[66,68]

Table 3 Comparison of available UAV simulators^[66,68]

Simulator	JMavSim	Gazebo	FlightGear	X-Plane	Air Sim
Commercial/free	Free	Free	Free	Commercial	Free
Interface ROS	Yes	Yes	No	No	No
Motion capture	No	No	No	No	Yes
Obstacles	No	Yes	Yes	Yes	Yes
MAVLink	Yes	Yes	Yes	Yes	Yes
Ease of Development	High	High	Medium	Medium	Medium

表 4 地面控制站软件的比较^[73-75]

Table 4 Comparison between GCS software^[73-75]

GCS software	QGroundControl	Mission Planner	MAVProxy
Interface	Graphical	Graphical	Command
Support MAVLink	Yes	Yes	Yes
Platform for Android	Yes	No	No
Pilot	PX4 Pro ArduPilot MAVLink compatible	ArduPilot PX4	ArduPilot MAVLink compatible

18.0 软件对无人机在悬停模式下的螺旋桨气流进行了气动流动模拟和实验验证。Marturano 等^[77]使用 COMSOL 软件中的流体动力学数值模拟来分析挂载在无人机上的探测器的最佳位置,研究无人机螺旋桨流的流体动力学和传感器位置对数据采集和调节的影响,以最大限度地提高无人机探测气体的能力。Ma 等^[78]结合实验,分析和研究了不同的无人机航速、转子组件结构、泄漏量和采样条件下无人机周围流场对气体采样的影响,通过仿真和实验确定了优化后的无人机装配结构和气敏传感器安装位置,并进行了验证。Roldán 等^[69]在四旋翼飞行器的仿真模型中增加了螺旋桨附近的细节设计,从而提高了仿真结果的精度,并减少了四旋翼飞行器其他部分的复杂性,进而降低了仿真计算成本。他们使用模拟软件 Autodesk Simulation CFD 2014 来确定四旋翼的空气动力学和转子的气流演变,并用一架四旋翼飞行器进行实验,验证了 CFD 模拟结果。流体动力学模拟的主要目的是优化无人机平台上气体传感器的位置,以最大限度地减少螺旋桨高速旋转产生的流场干扰,从而获得一个能够精确获取所需传感数据的最佳机载传感器系统。

目前公开报道了多种结合基于可调谐二极管激光吸收光谱技术的无人机天然气泄漏遥感探测仪^[79-81]。如图 8 所示,由美国宇航局(NASA)的喷气推进实验室(JPL)设计的微型可调谐激光光谱仪(TLS),采用一种发射近红外光的高效、超紧凑带间级联激光器,可以探测到 10^{-9} 量级的 CH_4 ,能够识别来自工业或自然来源的小型泄漏源^[82]。Khan 等^[83]验证了无人机挂载激光痕量气体传感器在大气边界层内测量大气温室气体分子浓度的可行性,设备照片如图 9 所示,其中轻型

紧凑的低功耗激光传感器由功率极低的垂直腔面发射激光器(VCSEL)、低功率驱动电子器件、圆柱形多通池,以及一个 InGaAs 光电探测器组成。3 台激光器的波长分别为 2001 nm、1651 nm 和 1854 nm,可以测量 CO_2 、 CH_4 和 H_2O 的分子浓度。传感器的质量为 2 kg,总功耗小于 3 W,内部多通池尺寸为 $20\text{ cm} \times 5\text{ cm} \times 5\text{ cm}$ 。传感器安装在型号为 T-Rex Align 700E 的垂直升降直升无人机上,其飞行时长为 20 min,有效载荷能力最高可达 68.6 N,垂直和水平分辨率均为 1 m,实现了大气边界层内温室气体的分子浓度测量。



图 8 无人机携带小型化的甲烷气体传感器^[82]

Fig. 8 A UAV carries a miniaturized methane gas sensor^[82]

Liu 等^[84]提出一种低成本的基于非色散红外技术的 CO_2 传感器,该传感器包括电池、气泵和干燥器,总质量为 1058 g,尺寸为 $15\text{ cm} \times 9.5\text{ cm} \times 11\text{ cm}$ 。将其装载在四旋翼无人机上,实现了大气中 CO_2 的测量,如图 10 所示。传感系统中气泵可加快气体交换,干燥机的作用是排除水汽的干扰,Raspberry Pi 作为机载计算机,将该传感系统集成到小型四旋翼无人机中,无人机可进行长达 30 min 的大气测量,在实验进行过程中精度保持在 1×10^{-6} (1σ) 以内。Chiba 等^[85]使用一台六旋翼无人机和一台非色散红外分析仪来检测区域内 CO_2 的分子浓度,如图 11 所示。该无人机载激光气体传感系统在 500、400、300、200、100、10 m 的高度飞行,获得 CO_2 的垂直分布图,结果表明, CO_2 的分子浓度随着飞行高度的增加而增大,长期测量后观测到的每月 CO_2 变化模式与气象局的 CO_2 变化规律相似,验证了该无人机载红外气体传感系统的长期稳定性。

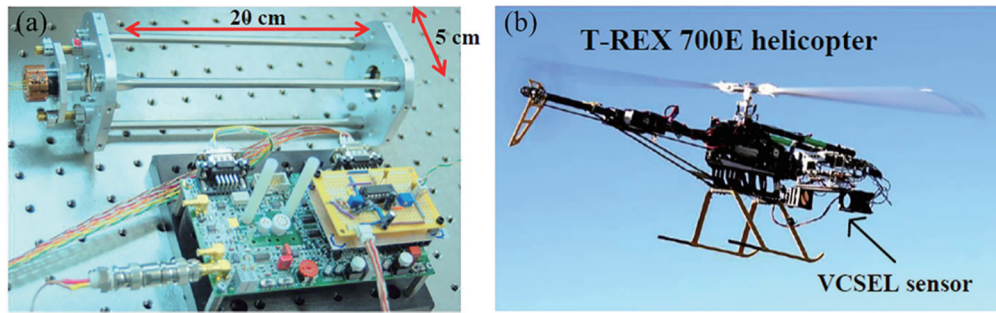


图 9 直升无人机气体传感平台^[83]。(a)垂直腔面发射激光传感器的多通池;(b)机载 VCSEL 传感器的直升无人机
Fig. 9 Photographs of the gas sensing platform based on a helicopter UAV^[83]. (a) Multi-pass cell in the vertical cavity surface emitting lasers sensor; (b) helicopter UAV with VCSEL sensor onboard

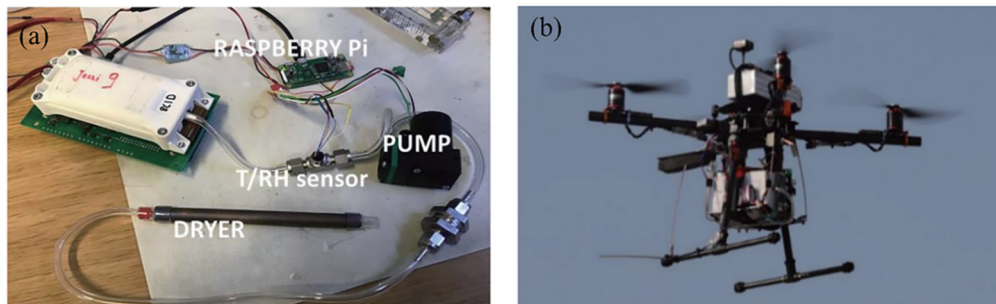


图 10 基于无人机的非分散红外气体传感器照片^[84]。(a)便携式 CO₂ 传感器系统的组成设备;(b)装载传感器的多旋翼无人机
Fig. 10 Photographs of non-dispersive infrared gas sensor based on UAV^[84]. (a) Components of the portable CO₂ sensor system setup; (b) selected multirotor UAV

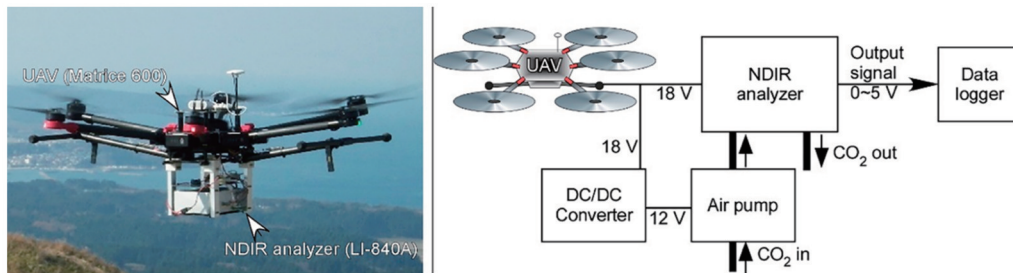


图 11 无人机载非分散红外气体监测平台的照片以及原理图^[85]
Fig. 11 Photograph and schematic of non-dispersive infrared gas monitoring platform based on UAV^[85]

5 结束语

从空气动力学原理、升降方式、尺寸性能 3 种分类方式对各类无人机平台展开了讨论,并对比了它们的性能。考虑到污染气体监测区域无人机的起飞环境,以及数据采集监测和时空分辨率的关系,将具有悬停和低速飞行性能的旋翼无人机用于激光气体监测是最优选择。旋翼无人机的续航时间短,这就需要无人机载激光传感器具有小体积、轻质量、低功耗的特点。针对这些特点,介绍了 4 种激光气体传感技术的基本原理和应用,它们都具有小型的传感器尺寸,很适合应用于无人机平台。另外,随着微电子技术的发展,激光的电流驱动板、温度控制板和信号处理电路也能够做到小体积和高精度,这就进一步推动了无人机载污染气

体激光监测平台向小型化和微型化发展。无人机监测技术的发展有利于完善中国“天地空”一体化立体监测体系,这对于中国参与全球环境治理和在应对气候变化国际合作领域发挥引领作用提供技术支撑,对中国建设美丽世界以及构建人类命运共同体具有积极的作用。

参 考 文 献

- [1] Nyquist J E. Unmanned aerial vehicles that even geoscience departments can afford[J]. Geotimes, 1997, 42(5): 20-23.
- [2] Quilter M C, Anderson V J. A proposed method for determining shrub utilization using (LA/LS) imagery[J]. Journal of Range Management, 2001, 54(4): 378-381.
- [3] Huang Y B, Thomson S J, Hoffmann C W, et al. Development and prospect of unmanned aerial vehicle technologies for agricultural production management[J]. International Journal of Agricultural and Biological Engineering, 2013, 6(3): 1-10.

- [4] Fornace K M, Drakeley C J, William T, et al. Mapping infectious disease landscapes: unmanned aerial vehicles and epidemiology[J]. *Trends in Parasitology*, 2014, 30(11): 514-519.
- [5] Kutnjak H, Leto J, Vranić M, et al. Potential of aerial robotics in crop production: high resolution NIR/VIS imagery obtained by automated unmanned aerial vehicle (UAV) in estimation of botanical composition of alfalfa-grass[EB/OL]. [2022-11-09]. https://bib.irb.hr/datoteka/752713.Potential_of_aerial_robotics_in_crop_production.pdf.
- [6] 巫阳, 罗涛, 刘常瑜, 等. 基于无人机探测大柴旦地区近地层气溶胶特征[J]. *光学学报*, 2022, 42(6): 0601003.
Wu Y, Luo T, Liu C Y, et al. UAV-based characteristic detection of near-surface layer aerosol over da Qaidam area[J]. *Acta Optica Sinica*, 2022, 42(6): 0601003.
- [7] Beard R, Kingston D, Quigley M, et al. Autonomous vehicle technologies for small fixed-wing UAVs[J]. *Journal of Aerospace Computing, Information, and Communication*, 2005, 2(1): 92-108.
- [8] Everaerts J. The use of unmanned aerial vehicles (UAVs) for remote sensing and mapping[J]. *The International Archives of the Photogrammetry, Remote Sensing and Spatial Information Sciences*, 2008, 37(2008): 1187-1192.
- [9] Kingston D, Beard R, McLain T, et al. Autonomous vehicle technologies for small fixed wing UAVs[C]//2nd AIAA "Unmanned Unlimited" Conf. and Workshop & Exhibit, September 15-18, 2003, San Diego, California. Virginia: AIAA Press, 2003: 6559.
- [10] Ben-Dor E, Patkin K, Banin A, et al. Mapping of several soil properties using DAIS-7915 hyperspectral scanner data—a case study over clayey soils in Israel[J]. *International Journal of Remote Sensing*, 2002, 23(6): 1043-1062.
- [11] Candiago S, Remondino F, De Giglio M, et al. Evaluating multispectral images and vegetation indices for precision farming applications from UAV images[J]. *Remote Sensing*, 2015, 7(4): 4026-4047.
- [12] Ehsani R, Sankaran S, Maja J M, et al. Affordable multi-rotor remote sensing platform for applications in precision horticulture [C/OL]//International Conference on Precision Agriculture, 2014 [2022-11-09]. https://www.ispag.org/abstract_papers/papers/abstract_1066.pdf.
- [13] Bryant R, Moran M S, McElroy S A, et al. Data continuity of Earth Observing 1 (EO-1) Advanced Land I satellite imager (ALI) and Landsat TM and ETM[J]. *IEEE Transactions on Geoscience and Remote Sensing*, 2003, 41(6): 1204-1214.
- [14] Lelong C C D, Burger P, Jubelin G, et al. Assessment of unmanned aerial vehicles imagery for quantitative monitoring of wheat crop in small plots[J]. *Sensors*, 2008, 8(5): 3557-3585.
- [15] Sampaio R C B, Hernandez A C, Becker M, et al. Novel hybrid electric motor glider-quadrotor MAV for in-flight/V-STOL launching[C]//2014 IEEE Aerospace Conference, March 1-8, 2014, Big Sky, MT, USA. New York: IEEE Press, 2014.
- [16] Ozdemir U, Aktas Y O, Vuruskan A, et al. Design of a commercial hybrid VTOL UAV system[J]. *Journal of Intelligent & Robotic Systems*, 2014, 74(1): 371-393.
- [17] Primicerio J, Di Gennaro S F, Fiorillo E, et al. A flexible unmanned aerial vehicle for precision agriculture[J]. *Precision Agriculture*, 2012, 13(4): 517-523.
- [18] Spanoudakis P, Doitsidis L, Tsourveloudis N, et al. Vertical takeoff and landing vehicle market overview[J/OL]. [2022-11-04]. https://www.researchgate.net/publication/265197693_Market_Overview_of_the_Vertical_Take-Off_and_Landing_Vehicles.
- [19] 谢家豪, 黄树彩, 韦道知, 等. 空天红外探测系统对无人机集群探测能力分析[J]. *光学学报*, 2022, 42(18): 1812002.
Xie J H, Huang S C, Wei D Z, et al. Analysis of detection ability of air-sky infrared detection system to UAV cluster[J]. *Acta Optica Sinica*, 2022, 42(18): 1812002.
- [20] Dong L, Yu Y J, Li C G, et al. Ppb-level formaldehyde detection using a CW room-temperature interband cascade laser and a miniature dense pattern multipass gas cell[J]. *Optics Express*, 2015, 23(15): 19821-19830.
- [21] Liu K, Wang L, Tan T, et al. Highly sensitive detection of methane by near-infrared laser absorption spectroscopy using a compact dense-pattern multipass cell[J]. *Sensors and Actuators B: Chemical*, 2015, 220: 1000-1005.
- [22] Cao Y C, Sanchez N P, Jiang W Z, et al. Simultaneous atmospheric nitrous oxide, methane and water vapor detection with a single continuous wave quantum cascade laser[J]. *Optics Express*, 2015, 23(3): 2121-2132.
- [23] 于欣, 李振钢, 刘家祥, 等. 基于积分球气室的光声光谱法气体检测研究[J]. *光学学报*, 2021, 41(16): 1612002.
Yu X, Li Z G, Liu J X, et al. Research on gas detection by photoacoustic spectroscopy based on integrating sphere gas cell [J]. *Acta Optica Sinica*, 2021, 41(16): 1612002.
- [24] Ren W, Luo L Q, Tittel F K. Sensitive detection of formaldehyde using an interband cascade laser near 3.6 μm [J]. *Sensors and Actuators B: Chemical*, 2015, 221: 1062-1068.
- [25] Li C G, Dong L, Zheng C T, et al. Compact TDLAS based optical sensor for ppb-level ethane detection by use of a 3.34 μm room-temperature CW interband cascade laser[J]. *Sensors and Actuators B: Chemical*, 2016, 232: 188-194.
- [26] Hassanalain M, Abdelkefi A. Classifications, applications, and design challenges of drones: a review[J]. *Progress in Aerospace Sciences*, 2017, 91: 99-131.
- [27] Hassanalain M, Abdelkefi A. Design, manufacturing, and flight testing of a fixed wing micro air vehicle with Zimmerman planform[J]. *Meccanica*, 2017, 52(6): 1265-1282.
- [28] Mueller T. Aerodynamic measurements at low Reynolds numbers for fixed wing micro-air vehicles[EB/OL]. [2022-11-09]. <https://www.semanticscholar.org/paper/Aerodynamic-Measurements-at-Low-Raynolds-Numbers-Mueller/11cf10cd4506f72c30da56ecdcc8fc2fa381cf92>.
- [29] Fenelon M A A, Furukawa T. Design of an active flapping wing mechanism and a micro aerial vehicle using a rotary actuator[J]. *Mechanism and Machine Theory*, 2010, 45(2): 137-146.
- [30] Shyy W, Lian Y, Tang J, et al. Aerodynamics of low Reynolds number flyers[M]. Cambridge: Cambridge University Press, 2008.
- [31] Shyy W, Aono H, Kang C K, et al. An introduction to flapping wing aerodynamics[M]. Cambridge: Cambridge University Press, 2013.
- [32] Joshi P M. Wing analysis of a flapping wing Unmanned aerial vehicle using CFD[J]. *Development*, 2015, 2(5): 216-221.
- [33] Schauwecker K, Ke N R, Scherer S A, et al. Markerless visual control of a quad-rotor micro aerial vehicle by means of on-board stereo processing[M]//Autonomous mobile systems 2012. Informatik aktuell. Heidelberg: Springer, 2012: 11-20.
- [34] Austin R. Unmanned aircraft systems: UAVS design, development and deployment[M]. Singapore: John Wiley & Sons Inc, 2010.
- [35] Singhal G, Bansod B, Mathew L. Unmanned aerial vehicle classification, applications and challenges: a review[EB/OL]. [2022-11-09]. <https://www.preprints.org/manuscript/201811.0601/v1>.
- [36] Watts A C, Ambrosia V G, Hinkley E A. Unmanned aircraft systems in remote sensing and scientific research: classification and considerations of use[J]. *Remote Sensing*, 2012, 4(6): 1671-1692.
- [37] Arjomandi M, Agostino S, Mammone M, et al. Classification of unmanned aerial vehicles[R]. Adelaide: University of Adelaide, 2006: 1-48.
- [38] Brooke-Holland L. Unmanned Aerial Vehicles (drones): an introduction[M]. London: House of Commons Library, 2012.

- [39] Weibel R, Hansman R J. Safety considerations for operation of different classes of UAVs in the NAS[C]//AIAA 4th Aviation Technology, Integration and Operations (ATIO) Forum, September 20-22, 2004, Chicago, Illinois. Virginia: AIAA Press, 2004: 6244.
- [40] 孙柳雅, 牛明生, 陈加雪, 等. 基于光声光谱技术的 NO₂ 探测[J]. 中国激光, 2022, 49(23): 2310002.
Sun L Y, Niu M S, Chen J X, et al. NO₂ detection based on photoacoustic spectroscopy technology[J]. Chinese Journal of Lasers, 2022, 49(23): 2310002.
- [41] Cui R Y, Dong L, Wu H P, et al. Generalized optical design of two-spherical-mirror multi-pass cells with dense multi-circle spot patterns[J]. Applied Physics Letters, 2020, 116(9): 091103.
- [42] Cui R Y, Dong L, Wu H P, et al. Three-dimensional printed miniature fiber-coupled multipass cells with dense spot patterns for ppb-level methane detection using a near-IR diode laser[J]. Analytical Chemistry, 2020, 92(19): 13034-13041.
- [43] Hodgkinson J, Smith R, Ho W O, et al. Non-dispersive infrared (NDIR) measurement of carbon dioxide at 4.2 μm in a compact and optically efficient sensor[J]. Sensors and Actuators B: Chemical, 2013, 186: 580-588.
- [44] Tittel F K, Curl R F, Dong L, et al. Recent advances in infrared semiconductor laser based chemical sensing technologies [M]//Pereira M F, Shulika O. Terahertz and mid infrared radiation. NATO science for peace and security series B: physics and biophysics. Dordrecht: Springer, 2011: 165-173.
- [45] Dong L, Kosterev A A, Thomazy D, et al. QEPAS spectrophones: design, optimization, and performance[J]. Applied Physics B, 2010, 100(3): 627-635.
- [46] Cui R Y, Dong L, Wu H P, et al. Calculation model of dense spot pattern multi-pass cells based on a spherical mirror aberration[J]. Optics Letters, 2019, 44(5): 1108-1111.
- [47] Dong L, Li C G, Sanchez N P, et al. Compact CH₄ sensor system based on a continuous-wave, low power consumption, room temperature interband cascade laser[J]. Applied Physics Letters, 2016, 108(1): 011106.
- [48] Cui R Y, Dong L, Wu H P, et al. Highly sensitive and selective CO sensor using a 2.33 μm diode laser and wavelength modulation spectroscopy[J]. Optics Express, 2018, 26(19): 24318-24328.
- [49] Wei T T, Zifarelli A, Dello Russo S, et al. High and flat spectral responsivity of quartz tuning fork used as infrared photodetector in tunable diode laser spectroscopy[J]. Applied Physics Reviews, 2021, 8(4): 041409.
- [50] Wei T T, Wu H P, Dong L, et al. Palm-sized methane TDLAS sensor based on a mini-multi-pass cell and a quartz tuning fork as a thermal detector[J]. Optics Express, 2021, 29(8): 12357-12364.
- [51] Mendes L B, Ogink N W M, Edouard N, et al. NDIR gas sensor for spatial monitoring of carbon dioxide concentrations in naturally ventilated livestock buildings[J]. Sensors, 2015, 15(5): 11239-11257.
- [52] Cutler S C, Vass A. Gas sensor: US 7541587 B2[P]. 2009-06-02.
- [53] Zosel J, Oelßner W, Decker M, et al. The measurement of dissolved and gaseous carbon dioxide concentration[J]. Measurement Science and Technology, 2011, 22(7): 072001.
- [54] Yin X K, Dong L, Wu H P, et al. Sub-ppb nitrogen dioxide detection with a large linear dynamic range by use of a differential photoacoustic cell and a 3.5 W blue multimode diode laser[J]. Sensors and Actuators B: Chemical, 2017, 247: 329-335.
- [55] Yin X K, Wu H P, Dong L, et al. Ppb-level SO₂ photoacoustic sensors with a suppressed absorption-desorption effect by using a 7.41 μm external-cavity quantum cascade laser[J]. ACS Sensors, 2020, 5(2): 549-556.
- [56] Kosterev A A, Buerki P R, Dong L, et al. QEPAS detector for rapid spectral measurements[J]. Applied Physics B, 2010, 100(1): 173-180.
- [57] Ma Y F. Review of recent advances in QEPAS-based trace gas sensing[J]. Applied Sciences, 2018, 8(10): 1822.
- [58] Patimisco P, Sampaolo A, Dong L, et al. Recent advances in quartz enhanced photoacoustic sensing[J]. Applied Physics Reviews, 2018, 5(1): 011106.
- [59] Tittel F K, Bakhirkin Y, Kosterev A, et al. Recent advances and applications of mid-infrared based trace gas sensor technology[J]. Proceedings of SPIE, 2008, 6900: 69000Z.
- [60] Li S Z, Lu J C, Shang Z J, et al. Compact quartz-enhanced photoacoustic sensor for ppb-level ambient NO₂ detection by use of a high-power laser diode and a grooved tuning fork[J]. Photoacoustics, 2022, 25: 100325.
- [61] Kosterev A, Wysocki G, Bakhirkin Y, et al. Application of quantum cascade lasers to trace gas analysis[J]. Applied Physics B, 2008, 90(2): 165-176.
- [62] Spagnolo V, Patimisco P, Sampaolo A, et al. Quartz-enhanced photoacoustic sensors for H₂S trace gas detection[J]. Proceedings of SPIE, 2015, 9370: 93700Y.
- [63] Li S Z, Dong L, Wu H P, et al. Ppb-level quartz-enhanced photoacoustic detection of carbon monoxide exploiting a surface grooved tuning fork[J]. Analytical Chemistry, 2019, 91(9): 5834-5840.
- [64] Wei T T, Wu H P, Dong L, et al. Acoustic detection module design of a quartz-enhanced photoacoustic sensor[J]. Sensors, 2019, 19(5): 1093.
- [65] Wu H P, Dong L, Zheng H D, et al. Beat frequency quartz-enhanced photoacoustic spectroscopy for fast and calibration-free continuous trace-gas monitoring[J]. Nature Communications, 2017, 8(1): 1-8.
- [66] Hentati A I, Krichen L, Fourati M, et al. Simulation tools, environments and frameworks for UAV systems performance analysis[C]//2018 14th International Wireless Communications & Mobile Computing Conference (IWCMC), June 25-29, 2018, Limassol, Cyprus. New York: IEEE Press, 2018: 1495-1500.
- [67] Li B, Feng C F, Wu H P, et al. Calibration-free mid-infrared exhaled breath sensor based on BF-QEPAS for real-time ammonia measurements at ppb level[J]. Sensors and Actuators B: Chemical, 2022, 358: 131510.
- [68] Perry A R. The FlightGear flight simulator[C]//Proceedings of the Annual Conference on USENIX Annual Technical Conference, June 27-July 2, 2004, Boston, MA, US. [S.l.: s. n.]. 2004, 686: 1-12.
- [69] Roldán J J, Joossen G, Sanz D, et al. Mini-UAV based sensory system for measuring environmental variables in greenhouses[J]. Sensors, 2015, 15(2): 3334-3350.
- [70] Ardupilot. Communicating with Raspberry Pi via MAVLink [EB/OL]. [2022-11-09]. <https://ardupilot.org/dev/docs/raspberry-pi-via-mavlink.html>.
- [71] Ardupilot. NVidia TX2 as a companion computer[EB/OL]. [2022-11-09]. <https://ardupilot.org/dev/docs/companion-computer-nvidia-tx2.html>.
- [72] Ardupilot. Communicating with ODroid via MAVLink[EB/OL]. [2022-11-09]. <https://ardupilot.org/dev/docs/odroid-via-mavlink.html>.
- [73] Dronecode. QGroundControl user guide[EB/OL]. [2022-11-09]. <https://docs.qgroundcontrol.com/en/>.
- [74] Ardupilot. Mission planner overview[EB/OL]. [2022-11-09]. <http://ardupilot.org/planner/docs/mission-planner-overview.html>.
- [75] Andreescu A M T, Dima M, Istrate A, et al. Autonomous system for image geo-tagging and target recognition[C/OL]//2nd International Workshop on Numerical Modelling in Aerospace Sciences, May 2014, Bucharest [2022-11-09]. <https://www.researchgate.net/publication/263562772>.

- [76] Li C Q, Han W T, Peng M M, et al. An unmanned aerial vehicle-based gas sampling system for analyzing CO₂ and atmospheric particulate matter in laboratory[J]. *Sensors*, 2020, 20(4): 1051.
- [77] Marturano F, Martellucci L, Chierici A, et al. Numerical fluid dynamics simulation for drones' chemical detection[J]. *Drones*, 2021, 5(3): 69.
- [78] Ma D L, Guo S C, Zhou Y X, et al. Optimization of sampling structure on UAV for gas leakage monitoring in the atmosphere [EB/OL]. [2022-11-09]. <https://europepmc.org/article/PPR/PPR465443>.
- [79] Barchyn T E, Hugenholtz C H, Myshak S, et al. A UAV-based system for detecting natural gas leaks[J]. *Journal of Unmanned Vehicle Systems*, 2017, 6(1): 18-30.
- [80] Abigail C, Brendan S. A study of a miniature TDLAS system onboard two unmanned aircraft to independently quantify methane emissions from oil and gas production assets and other industrial emitters[J]. *Atmosphere*, 2022, 13(5): 804.
- [81] Sebastian I, Piotr K, Marcin S, et al. Detection of natural gas leakages using a laser-based methane sensor and UAV[J]. *Remote Sensing*, 2021, 13(3): 510.
- [82] Patel P. Low-cost sensors could help natural gas producers plug costly methane leaks[J]. *ACS Central Science*, 2017, 26: 679-682.
- [83] Khan A, Schaefer D, Tao L, et al. Low power greenhouse gas sensors for unmanned aerial vehicles[J]. *Remote Sensing*, 2012, 4(5): 1355-1368.
- [84] Liu Y, Paris J D, Vrekoussis M, et al. Improvements of a low-cost CO₂ commercial nondispersive near-infrared (NDIR) sensor for unmanned aerial vehicle (UAV) atmospheric mapping applications[J]. *Atmospheric Measurement Techniques*, 2022, 15(15): 4431-4442.
- [85] Chiba T, Haga Y M, Inoue M, et al. Measuring regional atmospheric CO₂ concentrations in the lower troposphere with a non-dispersive infrared analyzer mounted on a UAV, Ogata village, Akita, Japan[J]. *Atmosphere*, 2019, 10(9): 487.

Advances in UAV Laser Monitoring Technology for Pollutant Gases

Wang Gang^{1,2}, Wu Hongpeng^{1,2}, Liao Jielin³, Wei Yongfeng³, Qiao Jianbo³, Dong Lei^{1,2*}

¹State Key Laboratory of Quantum Optics and Quantum Optics Devices, Institute of Laser Spectroscopy, Shanxi University, Taiyuan 030006, Shanxi, China;

²Collaborative Innovation Center of Extreme Optics, Shanxi University, Taiyuan 030006, Shanxi, China;

³Shanxi Dop Technology Co., Ltd., Taiyuan 030006, Shanxi, China

Abstract

Significance In China's "ground-air-space" integrated environmental monitoring platform, satellites are positioned in space to observe both atmospheric and terrestrial activities. Meanwhile, numerous air quality monitoring stations are established on the ground to complement the satellite observations. However, conventional monitoring platforms are insufficient in effectively covering the surface boundary layer, which ranges from 0.1 to 1 km above the ground. To this end, unmanned aerial vehicles (UAVs) with high mobility, moderate flight altitude, and easy deployment are employed for gas monitoring in the surface boundary layer when combined with gas sensors. One critical issue with the utilization of UAVs for gas sensing is their endurance, which poses a challenge for onboard gas sensors. These sensors should be small and lightweight with low power consumption to be carried on the UAVs. Currently, gas sensors employed for onboard applications are classified into four categories of electrochemical type, photoionization, catalytic combustion, and infrared sensing. Among them, the first three types of sensors are small, lightweight, and low-power, making them suitable for UAV payloads. However, they are generally less selective, which leads to difficulty in distinguishing target gases. In contrast, infrared sensors rely on the unique spectral fingerprint of gases to identify and detect target gases. When adopted with lasers, they exhibit high sensitivity, resolution, and selectivity, thus reducing measurement errors. As a result, infrared sensors are preferred for onboard gas sensing in UAVs, providing accurate and reliable measurements for monitoring air quality in the surface boundary layer.

The miniaturized sensing module based on laser absorption spectroscopy technology is highly suitable for UAV platforms. With the development of microelectronics technology, the lasers' current driving board, temperature control board, and signal processing circuit can realize the small size and high accuracy. This progress further promotes the miniaturization of UAV-based laser monitoring platforms for pollutant gases. UAV laser monitoring platforms can measure gases in the atmospheric boundary layer, thereby enhancing China's "ground-air-space" integrated monitoring platform. Consequently, a positive effect is produced on China's efforts to build a beautiful world and a community with a shared future for mankind.

Progress The UAV pollution gas laser monitoring platform comprises the UAV platform and the onboard laser sensor. Technological advancements have resulted in various UAV types with varying performance capabilities, which can cater to different task requirements (Fig. 1, Table 1). Pre-deployment tasks such as the availability of multiple UAV simulators,

onboard computers, and open-source ground stations guarantee the flight safety of the UAV platform during task execution (Tables 3-4). Gas sensors suitable for UAVs must be small and lightweight, with minimal power consumption. In trace gas monitoring, several miniature optical sensing modules based on laser absorption spectroscopy technology have been experimentally verified (Figs. 2-6, Table 2). To minimize the flow field interference created by high-speed propeller rotation and obtain the most accurate onboard sensor system for the required sensing data, we employ fluid dynamics simulation to optimize and analyze the turbulent distribution around the UAV. The combination of miniaturized laser gas sensors with UAVs has been applied in atmospheric air quality monitoring and natural gas leakage monitoring (Figs. 8-11). Such a combination can achieve three-dimensional measurements of time, space, and spectrum.

Conclusions and Prospects Our study provides an overview of current UAV platforms, including their types, advantages, disadvantages, and applications. It also highlights several principles and applications of laser spectroscopy sensing technologies suitable for UAVs. Additionally, we compare various open-source UAV simulators, onboard computers, and ground stations, and examine the challenges and solutions involved in integrating sensors with UAVs. The significant potential and value of employing small-scale laser sensors with UAVs in gas monitoring are also discussed. Finally, we emphasize the development direction for UAV-based pollution gas laser monitoring platforms, which is towards miniaturization and micro scale.

Key words laser spectroscopy; laser sensors; unmanned aerial vehicles; gas monitoring